THE MONOPOLE-DIMER MODEL ON CARTESIAN PRODUCTS OF PLANE GRAPHS

ANITA ARORA AND ARVIND AYYER

ABSTRACT. The monopole-dimer model is a signed variant of the monomer-dimer model which has determinantal structure. We extend the monopole-dimer model for planar graphs ($Math.\ Phys.\ Anal.\ Geom.,\ 2015$) to Cartesian products thereof and show that the partition function of this model can be expressed as a determinant of a generalised signed adjacency matrix. We then show that the partition function is independent of the orientations of the planar graphs so long as the orientations are Pfaffian. When these planar graphs are bipartite, we show that the computation of the partition function becomes especially simple. We then give an explicit product formula for the partition function of three-dimensional grid graphs a la Kasteleyn and Temperley-Fischer, which turns out to be fourth power of a polynomial when all grid lengths are even. Finally, we generalise this product formula to d dimensions, again obtaining an explicit product formula. We conclude with a discussion on asymptotic formulas for the free energy and monopole densities.

1. Introduction

The dimer model originally arose as the study of the physical process of adsorption of diatomic molecules (like oxygen) on the surface of a solid. Abstractly it can be thought of as enumerating perfect matchings in an edge-weighted graph. For planar graphs, Kasteleyn [Kas63] solved the problem completely by showing that the partition function can be written as a Pfaffian of a certain adjacency matrix built using a special class of orientations called Pfaffian orientations on the graph. An immediate corollary of Kasteleyn's result is that the Pfaffian is independent of the orientation. For the case of two-dimensional grid graphs $Q_{m,n}$, Kasteleyn [Kas61] and Temperley–Fisher [Fis61, TF61] independently gave an explicit product formula. For example, when m and n are even, horizontal (resp. vertical) edges have weight a (resp. b), the partition function can be written as

(1.1)
$$2^{mn/2} \prod_{i=1}^{m/2} \prod_{i=1}^{n/2} \left(a^2 \cos^2 \frac{i\pi}{m+1} + b^2 \cos^2 \frac{j\pi}{n+1} \right).$$

This formula is remarkable because although each factor is a degree-two polynomial in a and b with not-necessarily rational coefficients, the product turns out to be a polynomial with nonnegative integer coefficients. In particular, when a = b = 1, it is not obvious from this formula that the resulting product is an integer.

There have been attempts to generalise the dimer model while preserving this nice structure. The natural physical generalisation is the *monomer-dimer model*, which represents adsorption of

Date: April 30, 2024.

 $^{2010\} Mathematics\ Subject\ Classification.\ 82B20,\ 82B23,\ 05A15,\ 05C70.$

Key words and phrases. Monopole-dimer model, Cartesian products, Determinantal formula, Kasteleyn orientation, Bipartite, Cycle decomposition, Partition function, Grid graphs, Free energy.

a gas cloud consisting of both monoatomic and diatomic molecules. The abstract version here is the (weighted) enumeration of all matchings of a graph. The weights are interpreted as energies and are positive real numbers. This is known to be a computationally difficult problem [Jer87] and the partition function here does not have such a clean formula. However, when there is a single monomer on the boundary of a plane graph, the partition function can indeed be written as a Pfaffian [Wu06]. A lower bound for the partition function of the monomer-dimer model for d-dimensional grid graphs has been obtained by Hammersley–Menon [HM70] by generalising the method of Kasteleyn and Temperley–Fisher.

In another direction, a signed version of the monomer-dimer model called the monopole-dimer model has been introduced [Ayy15] for planar graphs. Configurations of the monopole-dimer model can be thought of as superpositions of two monomer-dimer configurations having monomers (called monopoles there) at the same locations. Thus, one ends up with even loops and isolated vertices. What makes the monopole-dimer model less physical is that configurations have a signed weight and they cannot be interpreted as energies anymore. On the other hand, the partition function here can be expressed as a determinant. Moreover, it is a perfect square for a $2m \times 2n$ grid graph. A combinatorial interpretation of the square root is given in [Ayy20].

In [Ayy15], a more general model called the *loop-vertex model* has also been defined for a general graph together with an orientation. The partition function in this case can also be written as a determinant. However, this model depends on the orientation. One of the main motivations for this work is to find natural families of non-planar graphs where the partition function is independent of the orientation, just as in the monopole-dimer model. The second motivation comes from the intuition that the monopole-dimer model is an 'integrable variant' of the more physical monomer-dimer model. If this is correct, asymptotic properties of both models should be similar. This has been explained in [Ayy15] for two dimensional grid. We expect this to hold for high-dimensional grids also. This is not easy to see because of the signs in monopole-dimer weights. We hope that our work will be a starting point towards establishing this relationship between the two models. We note in passing that higher dimensional dimer models have started attracting attention; see [CSW23, HLT23] for example.

We formulate the monopole-dimer model for Cartesian products of plane graphs in Section 3. A key ingredient in the formulation is the construction of special directed cycle decompositions of certain projections, which are themselves plane graphs with parallel edges. We first show in Theorem 3.8 that the partition function is a determinant of a generalised adjacency matrix built using Pfaffian orientations. As in the dimer model, we see immediately in Corollary 3.9 that the determinant is independent of the orientation. In Section 4, we focus attention on the monopole-dimer model on the Cartesian product of bipartite plane graphs. Here, we will show in Theorem 4.3 that we can allow arbitrary cycle decompositions of the projections mentioned above. This seems to be a new observation of independent interest.

We then focus on the special family of grid graphs in higher dimensions. We give an explicit product formula for the partition function of the monopole-dimer model on three-dimensional grid graphs in Theorem 5.1 generalising the expression (1.1). One peculiar feature of this partition function is that it is a fourth power of a polynomial when all side lengths are even. Just as for the partition function of the monopole-dimer model for two-dimensional grids, it would be interesting to obtain a combinatorial interpretation of the fourth root. We then briefly discuss the higher

dimensional case in Section 6 and give a similar explicit product formula in Theorem 6.1. We will also discuss its asymptotic behaviour in Section 7.

We begin with the background definitions and previous results.

2. Dimer Model

We begin by recalling basic terminology from graph theory. A (simple) graph is an ordered pair G = (V(G), E(G)), where V(G) is the set of vertices of G and E(G) is a collection of two-element subsets of V(G), known as edges. When we allow multiple edges between a pair of vertices (also called $parallel\ edges$), we will call such objects multigraphs. We will never allow self loops. We will work with undirected graphs and we will always assume that the graphs are finite and naturally vertex-labeled from $\{1,2,\ldots,|V(G)|\}$. A simple graph is therefore a graph with no parallel edges. All our models will be defined on simple graphs. We will encounter graphs with parallel edges only in certain decompositions. Recall that a planar graph is a graph which can be embedded in the plane, i.e. it can be drawn in such a way that no edges will cross each other. Such an embedding of a planar graph is referred as a $plane\ graph$ and it divides the whole plane into regions, each of which is called a face. We will consider only those embeddings of the graph for which parallel edges do not enclose any vertex. An orientation on a graph G is the assignment of arrows to its edges. A graph G with an orientation O is called an $oriented\ graph$ and is denoted (G, O). An orientation on a labeled graph obtained by orienting its edges from lower to higher labeled vertex is called a $canonical\ orientation$.

Definition 2.1. An orientation on a plane graph G is said to be Pfaffian if it satisfies the property that each simple loop enclosing a bounded face has an odd number of clockwise oriented edges. A Pfaffian orientation is said to possess the clockwise-odd property.

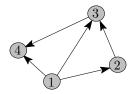


FIGURE 1. An oriented graph on 4 vertices.

For example, the orientation in Figure 1 is a Pfaffian orientation. Kasteleyn has shown that every plane graph has a Pfaffian orientation [Kas63]. A dimer covering or perfect matching is a collection of edges in the graph G such that each vertex is covered in exactly one edge. The set of all dimer coverings of G will be denoted as $\mathcal{M}(G)$. Let G be an edge-weighted graph on 2n vertices with real positive weight w_e for $e \in E(G)$ (thought of as the energy of e). Then the dimer model is the collection of all dimer coverings where the weight of each dimer covering $M \in \mathcal{M}(G)$ is given by $w(M) = \prod_{e \in M} w_e$. The partition function of the dimer model on G is then defined as

$$Z_G := \sum_{M \in \mathcal{M}(G)} w(M).$$

To state Kasteleyn's celebrated result, recall that a matrix $A = (a_{i,j})$ is skew-symmetric if $a_{i,j} = -a_{j,i}$ for every i, j, and the Pfaffian of $2n \times 2n$ skew-symmetric matrix A is given by

$$Pf(A) = \frac{1}{2^n n!} \sum_{\sigma \in S_{2n}} sgn(\sigma) A_{\sigma_1, \sigma_2} A_{\sigma_3, \sigma_4} \dots A_{\sigma_{2n-1}, \sigma_{2n}},$$

and Cayley's theorem [Cay49] says that for such a matrix, det $A = Pf(A)^2$.

Theorem 2.2 (Kasteleyn [Kas63]). If G is a plane graph with Pfaffian orientation \mathcal{O} , then the partition function of the dimer model on G is given by $Z_G = Pf(K_G)$, where K_G is a signed adjacency matrix defined by

$$(K_G)_{u,v} = \begin{cases} w_e & u \to v \text{ in } \mathcal{O}, \\ -w_e & v \to u \text{ in } \mathcal{O}, \\ 0 & \text{otherwise.} \end{cases}$$

Throughout this article, we will refer to cycles in configurations on graphs as loops. We will always understand these loops to be directed. Let us now recall generalization of the dimer model known as the loop-vertex model [Ayy15]. Let G be a simple weighted graph on n vertices with an orientation \mathcal{O} , vertex-weights x(v) for $v \in V(G)$ and edge-weights $a_{v,v'} \equiv a_{v',v}$ for $(v,v') \in E(G)$. A loop-vertex configuration C of G is a subgraph of G consisting of

- directed loops of even length (with length at least four),
- doubled edges (which can be thought of as loops of length two), and
- isolated vertices,

with the condition that each vertex of G is either an isolated vertex or is covered in exactly one loop. The set of all loop-vertex configurations of G will be denoted as $\mathcal{L}(G)$. Figure 2 shows a graph and two loop-vertex configurations on it.

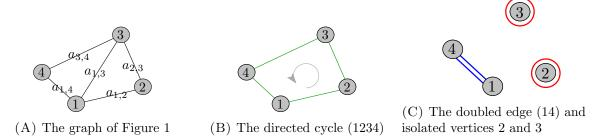


FIGURE 2. The graph of Figure 1 with edge weights marked in Figure 2(A), and two loop-vertex configurations on it in Figure 2(B) and Figure 2(C).

The sign of an edge $(v, v') \in E(G)$, is given by

(2.1)
$$\operatorname{sgn}(v, v') := \begin{cases} 1 & v \to v' \text{ in } \mathcal{O}, \\ -1 & v' \to v \text{ in } \mathcal{O}. \end{cases}$$

Let $\ell = (v_0, v_1, \dots, v_{2k-1}, v_{2k} = v_0)$ be a directed even loop in G. The weight of the loop ℓ is given by

(2.2)
$$w(\ell) := -\prod_{i=0}^{2k-1} \operatorname{sgn}(v_i, v_{i+1}) a_{v_i, v_{i+1}}.$$

Note that the weight of a doubled edge (v_i, v_j) is always $+a_{v_i,v_j}^2$.

Then the loop-vertex model on the pair (G, \mathcal{O}) is the collection $\mathcal{L}(G)$ with the weight of a configuration, $C = (\ell_1, \ldots, \ell_j; v_1, \ldots, v_k)$ consisting of loops ℓ_1, \ldots, ℓ_j and isolated vertices v_1, \ldots, v_k , given by

(2.3)
$$w(C) = \prod_{i=1}^{j} w(\ell_i) \prod_{i=1}^{k} x(v_i).$$

The (signed) partition function of the loop-vertex model is defined as

$$\mathcal{Z}_{G,\mathcal{O}} := \sum_{C \in \mathcal{L}(G)} w(C).$$

Example 2.3. Let G be a weighted graph on four vertices with vertex weights x for all the vertices and edge weights as shown in Figure 2(A). Then the weights of the configuration shown in Figures 2(B) and 2(C) are $a_{1,2}a_{2,3}a_{3,4}a_{1,4}$ and $x^2a_{1,4}^2$. The partition function of the loop-vertex model on the graph in Figure 2(A) with canonical orientation is

$$\mathcal{Z}_{G,\mathcal{O}} = x^4 + a_{1,2}^2 x^2 + a_{1,3}^2 x^2 + a_{1,4}^2 x^2 + a_{2,3}^2 x^2 + a_{3,4}^2 x^2 + a_{1,2}^2 a_{3,4}^2 + a_{1,4}^2 a_{2,3}^2 + 2a_{1,2} a_{2,3} a_{3,4} a_{1,4}.$$

Theorem 2.4. [Ayy15, Theorem 2.5] The partition function of the loop-vertex model on (G, \mathcal{O}) is

$$\mathcal{Z}_{G,\mathcal{O}} = \det \mathcal{K}_{G}$$

where K_G is a generalised adjacency matrix of (G, \mathcal{O}) defined as

(2.4)
$$\mathcal{K}_{G}(v,v') = \begin{cases} x(v) & v = v', \\ a_{v,v'} & v \to v' \operatorname{in} \mathcal{O}, \\ -a_{v,v'} & v' \to v \operatorname{in} \mathcal{O}, \\ 0 & (v,v') \notin E(G). \end{cases}$$

Example 2.5. The generalised adjacency matrix for the graph G in Example 2.3 with the canonical orientation is

$$\mathcal{K}_G = \begin{pmatrix} x & a_{1,2} & a_{1,3} & a_{1,4} \\ -a_{1,2} & x & a_{2,3} & 0 \\ -a_{1,3} & -a_{2,3} & x & a_{3,4} \\ -a_{1,4} & 0 & -a_{3,4} & x \end{pmatrix},$$

and

$$\det \mathcal{K}_G = x^4 + a_{1,2}^2 x^2 + a_{1,3}^2 x^2 + a_{1,4}^2 x^2 + a_{2,3}^2 x^2 + a_{3,4}^2 x^2 + a_{1,2}^2 a_{3,4}^2 + a_{1,4}^2 a_{2,3}^2 + 2a_{1,2} a_{2,3} a_{3,4} a_{1,4},$$
which is exactly $\mathcal{Z}_{G,\mathcal{O}}$ from Example 2.3.

If G is a simple vertex- and edge-weighted plane graph and \mathcal{O} is a Pfaffian orientation on it, then the loop-vertex model is called the *monopole-dimer model*. In that case, it has been shown [Ayy15, Theorem 3.3] that the weight of a loop $\ell = (v_0, v_1, \ldots, v_{2k-1}, v_{2k} = v_0)$ can be written as

(2.5)
$$w(\ell) = (-1)^{\text{number of vertices enclosed by } \ell} \prod_{j=0}^{2k-1} a_{v_j, v_{j+1}}.$$

Then Theorem 2.4 shows that the determinant of the generalised adjacency matrix of a plane graph with a Pfaffian orientation is independent of the latter.

3. Monopole-dimer model on Cartesian products of plane graphs

We now extend the definition of the monopole-dimer model to Cartesian products of plane graphs. The Cartesian product of two graphs G_1 and G_2 is the graph denoted $G_1 \square G_2$ with vertex set $V(G_1) \times V(G_2)$ and edge set

$$\left\{ ((u_1, u_2), (u'_1, u'_2)) \middle| \text{ either } u_1 = u'_1 \text{ and } (u_2, u'_2) \in E(G_2) \right\}.$$
or $u_2 = u'_2 \text{ and } (u_1, u'_1) \in E(G_1) \right\}.$

The above definition generalises to the Cartesian product of k graphs G_1, \ldots, G_k , denoted $G_1 \square \cdots \square G_k$. We will denote edges in $G_1 \square \cdots \square G_k$ of the form $((u_1, \ldots, u_i, \ldots, u_k), (u_1, \ldots, u_i', \ldots, u_k))$ G_i -edges. Recall that a path graph is a simple graph whose vertices can be arranged in a (non-repeating) linear sequence in such a way that two vertices are adjacent if and only if they are consecutive in the sequence. Clearly, a path graph is plane. Let P_n denote the path graph on n vertices. It is clear from the definition that the Cartesian product of k path graphs is a cuboid in \mathbb{Z}^k , also known as a grid graph. Figure 3 shows the Cartesian product $P_4 \square P_3$. We will use the notation [n] for the set $\{1, \ldots, n\}$.

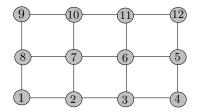


FIGURE 3. The Cartesian product $P_4 \square P_3$ with its boustrophedon labelling; see Section 5.

The degree of a vertex is the number of edges incident to it and an even graph G is one in which all the vertices have even degree. A walk in a graph G is a sequence $(v_0, e_1, v_1, \ldots, v_{t-1}, e_t, v_t)$ of alternating vertices v_0, \ldots, v_t and edges e_1, \ldots, e_t of G, such that v_{i-1} and v_i are the endpoints of e_i for $1 \leq i \leq t$. v_0 and v_t are called the *initial* and *final* vertices respectively. A path in G is a walk whose vertices and edges both are distinct. A cycle in G is a path whose initial and final vertices are identical. The size of a path or a cycle is the number of edges in it. The definitions in this paragraph apply also to multigraphs.

An edge-disjoint multiset of cycles in a multigraph G is a family of cycles $\mathcal{D} = \{d_1, \ldots, d_k\}$ such that no edge belongs in more than one cycle. In particular, a cycle decomposition of a multigraph G

is an edge-disjoint multiset of cycles \mathcal{D} of G such that $\bigcup_{d \in \mathcal{D}} E(d) = E(G)$. Veblen's theorem [BM08, Theorem 2.7] says that a multigraph admits a cycle decomposition if and only if it is even. We say that a cycle decomposition is *directed* if all of its cycles are directed. For a plane graph G and a cycle c in G, denote the number of vertices in V(G) enclosed by c as $\chi(c)$.

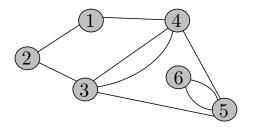
Definition 3.1. We say that the sign of an edge-disjoint multiset of directed cycles $\mathcal{D} = \{d_1, \ldots, d_k\}$ of an even plane multigraph G is given by

$$(3.1) \operatorname{sgn}(\mathcal{D}) := \prod_{i=1}^{k} \begin{cases} (-1)^{\chi(d_i)} & \text{if } d_i \text{ has odd size and is directed clockwise,} \\ (-1)^{\chi(d_i)+1} & \text{if either } d_i \text{ has even size, or has odd size} \\ & \text{and is directed anticlockwise.} \end{cases}$$

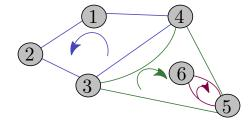
Note that this formula also defines the sign of a directed cycle decomposition.

Example 3.2. For the even plane graph H shown in Figure 4(A), the sign of its directed cycle decomposition $\{(1,2,3,4),(3,4,5),(5,6)\}$ shown in Figure 4(B) is

$$(-1)^{0+1} \times (-1)^1 \times (-1)^{0+1} = -1.$$



(A) A plane graph H with parallel edges



(B) H split as (1234)(345)(56)

FIGURE 4. (A) A plane graph on 6 vertices and (B) a directed cycle decomposition of it.

A trail in a multigraph G is a walk whose vertices can be repeated but edges are distinct. In particular, trails are allowed to self intersect at vertices. A $closed\ trail$ is one whose initial and terminal vertices are the same. Therefore, a closed trail can be decomposed into a edge-disjoint multiset of cycles. A $directed\ closed\ trail$ is a closed trail with a definite direction of traversal.

Definition 3.3. Let T be a directed closed trail in a multigraph G, We say that a directed cycle decomposition \mathcal{D} of T is compatible with T if the direction of cycles in \mathcal{D} is inherited from the direction of T.

Lemma 3.4. Let T be a closed directed trail in a plane multigraph G with Pfaffian orientation \mathcal{O} . Then all cycle decompositions of T compatible with it have the same sign.

Proof. The idea of this proof is similar to that of [Ayy15, Theorem 3.3]. Let $\mathcal{D} = \{d_1, \ldots, d_k\}$ be a directed cycle decomposition of T compatible with it. Then the number of edges of T oriented in

the opposite direction to T is given by

(3.2)
$$\sum_{j=1}^{k} \left(\text{number of edges oriented in opposite direction of } d_j \right).$$

For $j \in [k]$, let E_j and F_j be the number of edges and faces enclosed by d_j respectively. Since \mathcal{O} is Pfaffian, the number of clockwise oriented edges on the boundary of any bounded face f is odd (say O_f). Thus the number of clockwise oriented edges of d_j is

$$\sum_{\substack{f \text{ is a face in } G\\ \text{enclosed by } d_j}} O_f \, - E_j,$$

because each edge enclosed by d_j contributes to exactly two faces, one clockwise and one anticlockwise. Since O_f is odd for any bounded face f, the above quantity has the same parity as $F_j - E_j$. Now, using the Euler characteristic on the plane graph enclosed by d_j , the number of clockwise oriented edges of d_j and the number of vertices enclosed by d_j , which we called $\chi(d_j)$, have opposite parity. Thus the quantity in (3.2) is equal to $\operatorname{sgn}(\mathcal{D})$ given in (3.1).

Definition 3.5. The oriented Cartesian product of naturally labeled oriented graphs (G_1, \mathcal{O}_1) , \ldots , (G_k, \mathcal{O}_k) is the graph $G_1 \square \cdots \square G_k$ with orientation \mathcal{O} given as follows. For each $i \in [k]$, if $u_i \to u'_i$ in \mathcal{O}_i , then \mathcal{O} gives orientation $(u_1, \ldots, u_i, \ldots, u_k) \to (u_1, \ldots, u'_i, \ldots, u_k)$ if $u_{i+1} + u_{i+2} + \cdots + u_k + (k-i) \equiv 0 \pmod{2}$ and $(u_1, \ldots, u'_i, \ldots, u_k) \to (u_1, \ldots, u_i, \ldots, u_k)$ otherwise.

If we assign the canonical orientation to the graph in Figure 3, it can be thought of as an oriented Cartesian product of paths P_4 and P_3 which are labeled consecutively from one leaf to another.

Definition 3.6. The i-projection of a subgraph S of the Cartesian product $G_1 \square \cdots \square G_k$ is the multigraph obtained by contracting all but G_i -edges of S and is denoted \tilde{S}_i .

Let G_1, \ldots, G_k be k plane simple naturally labeled graphs and P be their Cartesian product. Let $\ell = (w_0, w_1, \ldots, w_{2s-1}, w_{2s} = w_0)$ be a directed even loop in P, and \mathcal{D}_i be a cycle decomposition compatible with the i-projection $\tilde{\ell}_i$. For $i \in [k]$, let $\hat{G}^{(i)}$ be the graph $G_1 \square \cdots \square G_{i-1} \square G_{i+1} \square \cdots \square G_k$. For $\hat{v} = (v_1, \ldots, v_{i-1}, v_{i+1}, \ldots, v_k) \in V(\hat{G}^{(i)})$, let $G_i(\hat{v})$ be the copy of G_i in P corresponding to \hat{v} and let $e_i(\hat{v})$ be the number of edges lying both in ℓ and $G_i(\hat{v})$. Now let

$$\begin{aligned} e_i &= \sum_{\substack{\hat{v} \in V(\hat{G}^{(i)}) \\ v_{i+1} + \dots + v_k + (k-i) \equiv 1 \pmod{2}}} e_i(\hat{v}). \end{aligned}$$

Then the sign of ℓ is defined by

(3.3)
$$\operatorname{sgn}(\ell) := -\prod_{i=1}^{k-1} (-1)^{e_i} \prod_{j=1}^k \operatorname{sgn}(\mathcal{D}_j).$$

Note that the sign of ℓ is well-defined by Lemma 3.4. Now suppose that P has been given vertex weights x(w) for $w \in V(P)$ and edge weights a_e for $e \in E(P)$. Then the weight of the loop ℓ is defined as

(3.4)
$$w(\ell) := \operatorname{sgn}(\ell) \prod_{e \in E(\ell)} a_e.$$

Note that the orientation of a graph G is not relevant for the definition of the loop-vertex configuration (defined in Section 2) on G. We will call a loop-vertex configuration an *(extended) monopole-dimer configuration* when the underlying graph G is a Cartesian product of simple plane graphs.

Definition 3.7. The (extended) monopole-dimer model on the weighted Cartesian product $P = G_1 \square \cdots \square G_k$ is the collection \mathcal{L} of monopole-dimer configurations on P where the weight of each configuration $C = (\ell_1, \ldots, \ell_m; v_1, \ldots, v_n)$ given by

$$w(C) = \prod_{i=1}^{m} w(\ell_i) \prod_{i=1}^{n} x(v_i).$$

The (signed) partition function of the monopole-dimer model on the Cartesian product P is

$$\mathcal{Z}_P := \sum_{C \in \mathcal{L}} w(C).$$

From the above definition, it is clear that \mathcal{Z}_P is independent of the orientations on G_1, \ldots, G_k . The following result is a generalisation of Theorem 2.4 when G is plane and \mathcal{O} is Pfaffian. Recall that \mathcal{K}_P is the generalised adjacency matrix defined in (2.4) for (P, \mathcal{O}) .

Theorem 3.8. Let G_1, \ldots, G_k be k simple plane naturally labeled graphs with Pfaffian orientations $\mathcal{O}_1, \ldots, \mathcal{O}_k$ respectively. The (signed) partition function of the monopole-dimer model for the weighted oriented Cartesian product (P, \mathcal{O}) of G_1, \ldots, G_k is given by

$$(3.5) \mathcal{Z}_P = \det \mathcal{K}_P.$$

The proof strategy is similar to that of Theorem 2.4.

Proof. Since \mathcal{K}_P is the sum of a diagonal matrix and an antisymmetric matrix, the only terms contributing to $\det \mathcal{K}_P$ correspond to permutations which are product of even cycles and singletons, and hence are in bijective correspondence with monopole-dimer configurations on P. Thus, we only need to show that sign coming from an even cyclic permutation $(v_0, v_1, \ldots, v_{2s-1}, v_{2s} = v_0)$ coincides with the sign of the corresponding directed loop $\ell = (v_0, v_1, \ldots, v_{2s-1}, v_{2s} = v_0)$. That is, we have to prove that

$$(-1)^{\text{\#edges pointing in opposite direction of } \ell \text{ (under } \mathcal{O})+1} = \operatorname{sgn} \ell.$$

Let r be the number of edges pointing in opposite direction of ℓ under \mathcal{O} . Note that the contribution to r comes from k type of edges, G_1 -edges, G_2 -edges,..., G_k -edges in ℓ . Since ℓ is a directed cycle, the i-th projection $\tilde{\ell}_i$, of ℓ is a directed trail in \tilde{P}_i (which is just G_i with multiple edges). Let $\mathcal{D}_i = \{d_{i,1}, d_{i,2}, \ldots, d_{i,m_i}\}$ be a directed cycle decomposition compatible with $\tilde{\ell}_i$ according to Definition 3.3. Denote the number of edges in $d_{i,j}$, for $j \in [m_i]$, oriented under \mathcal{O} in the direction opposite to it as $\varepsilon^{i,j}$.

Recall the notation $\chi(c)$ and e_i from earlier in this section. For $i \in [k-1]$, the edges contributing to e_i have been reversed while defining \mathcal{O} and thus the contribution of G_i -edges to r is

$$\sum_{j=1}^{m_i} \varepsilon^{i,j} \equiv e_i$$

$$+ \sum_{i=1}^{m_i} (\text{number of edges in } d_{i,j} \text{ oriented under } \mathcal{O}_i \text{ in the direction opposite to it}) \pmod{2}.$$

By the proof of Lemma 3.4, it follows that the number of clockwise oriented edges of $d_{i,j}$ under \mathcal{O}_i and $\chi(d_{i,j})$ have opposite parity. Therefore,

$$\sum_{j=1}^{m_i} \varepsilon^{i,j} \equiv e_i + \sum_{j=1}^{m_i} \begin{cases} \chi(d_{i,j}) & \text{if } d_{i,j} \text{ has odd size} \\ & \text{and is directed clockwise,} \\ \chi(d_{i,j}) + 1 & \text{if either } d_{i,j} \text{ has even size, or has odd size} \\ & \text{and is directed anticlockwise.} \end{cases}$$
 (mod 2).

Now, by Definition 3.1, G_i -edges of ℓ contribute $(-1)^{e_i}$ sgn \mathcal{D}_i to $(-1)^r$. Similarly, the contribution of G_k -edges to $(-1)^r$ is sgn \mathcal{D}_k as we have not altered the directions coming from \mathcal{O}_k in any copy of G_k . Thus,

$$(-1)^r = \prod_{i=1}^{k-1} (-1)^{e_i} \operatorname{sgn} \mathcal{D}_i \times \operatorname{sgn} \mathcal{D}_k = \prod_{i=1}^{k-1} (-1)^{e_i} \prod_{s=1}^k \operatorname{sgn} \mathcal{D}_s,$$

resulting in $(-1)^{r+1} = \operatorname{sgn} \ell$. Hence, we get the (signed) partition function of the (extended) monopole-dimer model for the oriented cartesian product as a determinant.

Recall that the partition function of the monopole-dimer model is defined for (unoriented) Cartesian product of graphs in Definition 3.7. The next result can thus be seen as an analogue of the observation made at the end of Section 2.

Corollary 3.9. Let G_1, \ldots, G_k be k simple plane naturally labeled graphs with Pfaffian orientations $\mathcal{O}_1, \ldots, \mathcal{O}_k$ respectively. Then the determinant of the generalised adjacency matrix \mathcal{K}_P of the oriented cartesian product, (P, \mathcal{O}) , of $(G_1, \mathcal{O}_1), \ldots, (G_k, \mathcal{O}_k)$ is independent of the Pfaffian orientations $\mathcal{O}_1, \ldots, \mathcal{O}_k$.

4. Monopole-dimer model on Cartesian products of plane bipartite graphs

Recall that a bipartite graph is a graph G whose vertex set can be partitioned into two subsets X and Y such that each edge of G has one end in X and other end in Y. Bipartite graphs only have cycles of even length. Since the direction of even cycles does not affect the sign in Definition 3.1, we can write the sign of an edge-disjoint multiset of cycles $\mathcal{D} = \{d_1, \ldots, d_k\}$ in an even bipartite plane multigraph G as $sgn(\mathcal{D}) := \prod_{i=1}^k (-1)^{\chi(d_i)+1}$.

Note that the above formula also applies to a cycle decomposition of an even bipartite plane multigraph. We will show that the sign of a cycle decomposition remains the same for all cycle decompositions of a plane bipartite even multigraph. For that we first define some moves on two cycles in a decomposition.

Let G be an even plane bipartite multigraph and (c_1, \ldots, c_t) be an edge-disjoint multiset of cycles in G. Then we define the following moves transforming one multiset of cycles into another. For each move, we also calculate the change in the sign of this multiset of cycles.

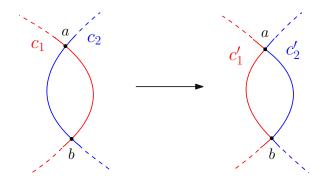


FIGURE 5. The M_1 -move from Item 1. Here, the dotted blue and red lines indicate that they are allowed to intersect each other.

(1) The M_1 -move changes cycles c_1 , c_2 into cycles c'_1 , c'_2 as shown in Figure 5. Let v (resp. v') be the number of internal vertices lying on the blue (resp. red) solid path from a to b along c_2 (resp. c_1) in the left side of Figure 5. Let u be the number of vertices enclosed by the cycle formed by these two paths. Then

$$\chi(c'_1) + \chi(c'_2) = \chi(c_1) - u - v + \chi(c_2) - u - v'$$

$$\equiv \chi(c_1) + \chi(c_2) \pmod{2}$$

$$\equiv (\chi(c_1) + 1) + (\chi(c_2) + 1) \pmod{2},$$

where we have used the fact that $v + v' \equiv 0$ (as G is bipartite) in the second line. Thus, performing the M_1 -move in this multiset of cycles preserves its sign.

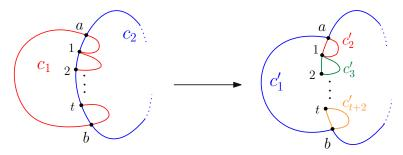


FIGURE 6. The M_2 -move from Item 2. The dotted arc of c_2 on the right indicates that it can intersect with the part of c_1 from a to b on the right side.

(2) Let c_1, c_2 intersect as shown on the left side of Figure 6. Without loss of generality, the left arc of c_1 strictly between a and b does not intersect c_2 , and the right arc of c_1 strictly between a and b only at the t points shown. The M_2 -move changes cycles c_1, c_2 into (t+2) cycles $c'_1, c'_2, \ldots, c'_{t+2}$ as shown in

the right side of Figure 6. Then, by considering internal vertices in all regions, the sign of the latter multiset is given by

$$\sum_{i=1}^{t+2} (\chi(c_i') + 1) = \chi(c_1') + \sum_{i=2}^{t+2} \chi(c_i') + (t+2)$$

$$= \left(\chi(c_1) + \chi(c_2) + t - \sum_{i=2}^{t+2} \chi(c_i')\right) + \sum_{i=2}^{t+2} \chi(c_i') + t + 2$$

$$\equiv (\chi(c_1) + 1) + (\chi(c_2) + 1) \pmod{2}.$$

Thus, the M_2 -move also preserves the sign of the multiset of cycles.

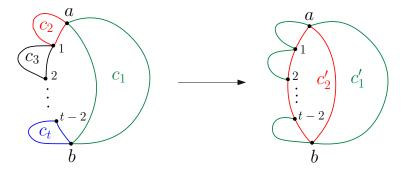


FIGURE 7. The M_3 -move from Item 3.

(3) For $t \geq 2$, suppose c_1, \ldots, c_t are cycles in the multigraph G such that they form a closed chain as shown on the left side in Figure 7. Note that these cycles do not intersect at points other than those shown in the figure. The M_3 -move converts these t cycles into two cycles namely c'_1, c'_2 as shown in the right side of Figure 7. Then the sign of the latter multiset of cycles is

$$\sum_{i=1}^{2} (\chi(c_i') + 1) \equiv \chi(c_1') - \chi(c_2') \pmod{2},$$

$$\equiv \sum_{i=1}^{t} \chi(c_i) + (\text{size of } c_2') - t \pmod{2},$$

because c_1' encloses all the vertices except $a, b, 1, \ldots, (t-2)$ lying on c_2' . Since G is bipartite, it can only have cycles of even size. Thus

$$\sum_{i=1}^{2} (\chi(c_i') + 1) \equiv \sum_{i=1}^{t} \chi(c_i) + t \pmod{2}$$
$$\equiv \sum_{i=1}^{t} (\chi(c_i) + 1) \pmod{2}.$$

Again, the sign of the multiset is preserved under the M_3 -move.

We have thus shown that performing any sequence of moves of the form Items 1, 2 and 3 will not affect the sign of a multiset of cycles.

Recall that a *bridge* or *cut edge* in a multigraph G is an edge whose deletion increases the number of connected components in G. Let G be a connected even plane multigraph. Then G cannot have a bridge [BM08, Exercise 3.2.3] and hence the boundary of the outer face (being a closed trail) can be decomposed into cycles c_1, \ldots, c_k such that $|V(c_i) \cap V(c_i)| \leq 1$ for all $i, j \in [k]$.

Definition 4.1. Let G be a connected even plane multigraph and C be the boundary of the outer face consisting of cycles c_1, \ldots, c_k . Then an outer cycle decomposition of G is a cycle decomposition of G containing c_1, \ldots, c_k and the latter will be called boundary cycles.

The next result is a crucial step towards the main result of this section.

Lemma 4.2. Let G be a connected bipartite even plane multigraph. Then for any cycle decomposition \mathcal{D} of G, there exists an outer cycle decomposition \mathcal{D}' of G with same sign.

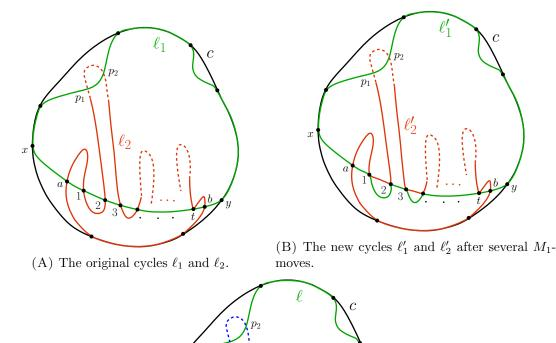
Proof. Suppose c_1, \ldots, c_k are the boundary cycles. If k > 1, we can work separately with each subgraph of G lying inside the cycle c_j for each $j \in [k]$. Thus, without loss of generality, we can assume that there is just a single cycle c (say). If \mathcal{D} contains c, there is nothing to prove. So assume \mathcal{D} does not contain c. Then there exist at least two cycles in \mathcal{D} which will intersect c in some edge(s). There are two possibilities now depending on whether the cycles above intersect each other more than once or not.

- (1) If there are two cycles among these, say ℓ_1 and ℓ_2 , which intersect each other in more than one point, say a and b, then ℓ_1, ℓ_2 will look as in Figure 8(A). Let the bottom arc of ℓ_1 joining x to y intersect ℓ_2 in t additional points as shown. First perform the necessary number of M_1 -moves to reach the stage in Figure 8(B). At this point, the top part of the ℓ'_2 cycle between a and b lies on the same side of the bottom part of the ℓ'_1 cycle. Now, perform an M_2 -move to increase the number of edges of c covered by ℓ'_1 as depicted in Figure 8(C). Since these moves preserve the sign, the cycle decomposition containing (t+2) transformed cycles in place of two original cycles will have the same sign.
- (2) If no two cycles of \mathcal{D} which have a common edge with c intersect each other in more than one point, then we have a certain number, say $t \geq 3$, of cycles intersecting c. Focus on one of the cycles, ℓ_1 say. It will intersect another cycle at a vertex of c. Call it ℓ_2 . Now following ℓ_1 in the interior, find the first of these t cycles and call it ℓ_t . The situation will look as in left of Figure 9. Now perform an M_3 -move to increase the number of edges of c covered by ℓ_1 and arrive at the right of Figure 9. The resulting cycle decomposition will have the same sign.

Apply these cases inductively. Notice that we might need to alternate between these two. In each case, the number of edges in the intersection of ℓ_1 and c increases. As the number of edges in c is finite, the process of performing these moves will eventually stop and we will end up with a cycle decomposition containing c with the sign same as that of \mathcal{D} .

Now we will see a result analogous to Lemma 3.4 in the case of bipartite graphs.

Theorem 4.3. Let G be a connected bipartite even plane multigraph. Then all cycle decompositions \mathcal{D} of G will have same sign.

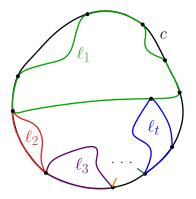


(C) The final cycles after an M_2 -move. Note that there are a total of t+2 cycles now.

FIGURE 8. Two cycles ℓ_1 and ℓ_2 intersecting the boundary cycle c, and intersecting each other in more than one point in Figure 8(A). In Figure 8(C), the cycle ℓ intersects c in more edges than ℓ_1 .

Proof. Since G is even and connected, the boundary of the outer face of G can be decomposed into cycles. For simplicity, we suppose the boundary is a single cycle c. If not, the argument below extends in an obvious way to each component of the boundary.

Let \mathcal{D} be a cycle decomposition of G. Using Lemma 4.2, we obtain another cycle decomposition \mathcal{D}_1 containing c which has the same sign as \mathcal{D} . Let G_1 be obtained from G by removing all the edges of c and the resulting isolated vertices. Note that although G_1 can be disconnected, the regions enclosed by its connected components $G_{1,1}, G_{1,2}, \ldots, G_{1,t}$ will not intersect. Now, $\mathcal{D}_1 \setminus \{c\}$ is a cycle decomposition of G_1 . Again using Lemma 4.2 on G_1 , we obtain a cycle decomposition \mathcal{D}_2 of G containing c and $d_{1,1}, d_{1,2}, \ldots, d_{1,t}$, the boundary cycles of $G_{1,1}, G_{1,2}, \ldots, G_{1,t}$ respectively,



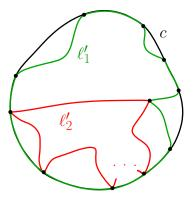


FIGURE 9. A cycle decomposition where the cycles intersecting the boundary cycle are shown before and after an M_3 -move.

such that $\operatorname{sgn} \mathcal{D}_1 = \operatorname{sgn} \mathcal{D}_2$. Now remove $d_{1,1}, d_{1,2}, \ldots, d_{1,t}$ from G_1 to obtain G_2 and continue this process. Since G is finite, this process must stop. In fact, it will stop at the cycle decomposition obtained by successively including outer boundaries of G_1, G_2 and so on.

Recall the *i*-projection, the sign of a directed loop and the notation e_i defined in Definition 3.6, (3.3) and Section 3 respectively. By the fact that bipartite graphs only have even cycles and by Theorem 4.3, we have the following result.

Corollary 4.4. Let G_1, \ldots, G_k be plane simple naturally labeled bipartite graphs and P be their Cartesian product. Let $\ell = (w_0, w_1, \ldots, w_{2s-1}, w_{2s} = w_0)$ be a directed even loop in P and \mathcal{D}_i be an arbitrary cycle decomposition of the i-projection $\tilde{\ell}_i$ for $i \in [k]$. Then

$$\operatorname{sgn}(\ell) = -\prod_{i=1}^{k-1} (-1)^{e_i} \prod_{j=1}^{k} \operatorname{sgn}(\mathcal{D}_j),$$

and is well-defined. In particular, there is no restriction on the choice of cycle decomposition of any i-projection in the monopole-dimer model for Cartesian product of bipartite graphs.

5. Three-dimensional grids

Recall that P_n is the path graph on n vertices. Assign to P_n the natural labelling increasing from one leaf to another, and denote its oriented variant with the canonical orientation as (P_n, \mathcal{O}_n) . Consider the two-dimensional grid graph $P_\ell \Box P_m = \{(p,q) \mid p \in [\ell], q \in [m]\}$ whose vertex (p,q) has label $2s\ell + p$ if q = 2s + 1 and $2s\ell - p + 1$ if q = 2s. Such a 'snake-like' labelling is known as a boustrophedon labelling [HM70]. Figure 3 shows this labelling on $P_4 \Box P_3$. With the canonical orientation, denote this graph as $(P_\ell \Box P_m, \mathcal{O}_{\ell,m})$. For the purposes of our next result, we will think of the Cartesian product of $P_\ell \Box P_m$ with P_n as embedded in \mathbb{Z}^3 where the coordinate axes x, y, z are aligned parallel to the edges in P_ℓ , P_m and P_n respectively.

Theorem 5.1. Let (G, \mathcal{O}) be the oriented Cartesian product of $(P_{\ell} \Box P_m, \mathcal{O}_{\ell,m})$ with (P_n, \mathcal{O}_n) . Let vertex weights be x for all vertices of G, and edge weights be a, b, c for the edges along the three

coordinate axes. Then the partition function of the monopole-dimer model on G is given by

$$\mathcal{Z}_{G} \equiv \mathcal{Z}_{\ell,m,n} = \prod_{j=1}^{\lfloor n/2 \rfloor} \prod_{s=1}^{\lfloor m/2 \rfloor} \prod_{k=1}^{\lfloor \ell/2 \rfloor} \left(x^{2} + 4a^{2} \cos^{2} \frac{\pi k}{\ell+1} + 4b^{2} \cos^{2} \frac{\pi s}{m+1} + 4c^{2} \cos^{2} \frac{\pi j}{n+1} \right)^{4}$$

$$\times \begin{cases} 1 & \ell, n, m \in 2\mathbb{N}, \\ T_{n,m}^{2}(b,c;x) & \ell \notin 2\mathbb{N}, m, n \in 2\mathbb{N}, \\ T_{n,m}^{2}(b,c;x) & \ell, n \in 2\mathbb{N}, m \notin 2\mathbb{N}, \\ T_{n,m}^{2}(b,c;x) & T_{n,\ell}^{2}(a,c;x) & \ell, m \notin 2\mathbb{N}, n \in 2\mathbb{N}, \\ T_{m,\ell}^{2}(a,b;x) & \ell, m \in 2\mathbb{N}, n \notin 2\mathbb{N}, \\ T_{n,m}^{2}(b,c;x) & T_{m,\ell}^{2}(a,b;x) & \ell, n \notin 2\mathbb{N}, n \notin 2\mathbb{N}, \\ T_{n,\ell}^{2}(a,c;x) & T_{m,\ell}^{2}(a,b;x) & \ell, n \notin 2\mathbb{N}, m \in 2\mathbb{N}, \\ T_{n,\ell}^{2}(a,c;x) & T_{n,\ell}^{2}(a,b;x) & \ell \in 2\mathbb{N}, m, n \notin 2\mathbb{N}, \\ T_{n,\ell}^{2}(a,c;x) & T_{n,\ell}^{2}(a,c;x) & T_{m,\ell}^{2}(a,b;x) & \ell \in 2\mathbb{N}, m, n \notin 2\mathbb{N}, \end{cases}$$

where

$$S_n(c;x) = \prod_{k=1}^{\lfloor n/2 \rfloor} \left(x^2 + 4c^2 \cos^2 \frac{\pi k}{n+1} \right),$$

and

$$T_{n,\ell}(a,b;x) = \prod_{j=1}^{\lfloor n/2 \rfloor} \prod_{k=1}^{\lfloor \ell/2 \rfloor} \left(x^2 + 4a^2 \cos^2 \frac{\pi k}{\ell+1} + 4b^2 \cos^2 \frac{\pi j}{n+1} \right).$$

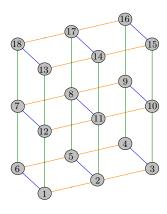


FIGURE 10. The boustrophedon labelling on $P_3 \square P_2 \square P_3$.

Remark 5.2. The boustrophedon labelling that induces the orientation \mathcal{O} over the graph G is as follows. The vertex (p,q,r) has label

$$\begin{cases} 2t\ell m + 2s\ell + p & q = 2s+1, r = 2t+1, \\ 2t\ell m + 2s\ell - p + 1 & q = 2s, r = 2t+1, \\ 2t\ell m - 2s\ell - p + 1 & q = 2s+1, r = 2t, \\ 2t\ell m - 2s\ell + p & q = 2s, r = 2t, \end{cases}$$

where $p \in [\ell], q \in [m]$ and $r \in [n]$. Figure 10 shows this labelling on the graph $P_3 \square P_2 \square P_3$.

Proof. The signed adjacency matrix for the graph (G, \mathcal{O}) with the above labelling can be written as

$$(5.1) \mathcal{K}_{\ell,m,n} = I_n \otimes I_m \otimes T_{\ell}(-a,x,a) + I_n \otimes T_m(-b,0,b) \otimes J_{\ell} + T_n(-c,0,c) \otimes J_m \otimes J_{\ell},$$

where $T_k(-s, z, s)$ is the $k \times k$ tridiagonal Toeplitz matrix with diagonal entries z, subdiagonal entries -s and superdiagonal entries s. Let J_k be the $k \times k$ antidiagonal matrix with all antidiagonal entries equal to 1 and let $\iota = \sqrt{-1}$. Transform $T_k(-s, z, s)$ into the diagonal matrix

$$D_k = \operatorname{diag}\left(z + 2\iota s \cos\frac{\pi}{k+1}, \dots, z + 2\iota s \cos\frac{k\pi}{k+1}\right)$$

using the standard unitary similarity transformation [Fis61, Section 4] given by the matrix u_k whose entries are given by $(u_k)_{p,q} = \sqrt{\frac{2}{k+1}} \iota^p \sin(\pi pq/(k+1))$. A short calculation shows that

(5.2)
$$(u_k)^{-1} J_k u_k = \iota^{k-1} \begin{pmatrix} & & (-1)^{k-1} \\ & & (-1)^{k-2} \\ & \ddots & \\ (-1)^0 & & \end{pmatrix}.$$

Let \sim denote the equivalence relation on matrices given by similarity. Then, using the unitary transform $u_n \otimes u_m \otimes u_\ell$, we find that

$$\mathcal{K}_{\ell,m,n} \sim I_n \otimes I_m \otimes \operatorname{diag}\left(x + 2\iota a \cos\frac{\pi}{\ell+1}, \dots, x + 2\iota a \cos\frac{\ell\pi}{\ell+1}\right) \\
+ I_n \otimes 2\iota b \operatorname{diag}\left(\cos\frac{\pi}{m+1}, \dots, \cos\frac{m\pi}{m+1}\right) \otimes \iota^{\ell-1} \begin{pmatrix} & (-1)^{\ell-1} \\ & \ddots & \\ & & (-1)^0 \end{pmatrix} \\
+ 2\iota c \operatorname{diag}\left(\cos\frac{\pi}{n+1}, \dots, \cos\frac{n\pi}{n+1}\right) \\
\otimes \iota^{m-1} \begin{pmatrix} & (-1)^{m-1} \\ & \ddots & \\ & & (-1)^0 \end{pmatrix} \otimes \iota^{\ell-1} \begin{pmatrix} & (-1)^{\ell-1} \\ & \ddots & \\ & & (-1)^0 \end{pmatrix}.$$

Note that each term in the above sum is a block diagonal matrix as the first matrix in each tensor factor is diagonal. Therefore, $\mathcal{K}_{\ell,m,n}$ is similar to an $n \times n$ block diagonal matrix with the block F_j

for $j \in [n]$ given by

Define

$$\lambda_{s,j}^{m,n} = \sqrt{4b^2 \cos^2 \frac{s\pi}{m+1} + 4c^2 \cos^2 \frac{j\pi}{n+1}}, \quad s \in [m], j \in [n],$$

and let

$$D_{j} = \begin{cases} \operatorname{diag}\left(\iota\lambda_{1,j}^{m,n}, -\iota\lambda_{1,j}^{m,n}, \iota\lambda_{2,j}^{m,n}, -\iota\lambda_{2,j}^{m,n}, \dots, \iota\lambda_{\frac{m}{2},j}^{m,n}, -\iota\lambda_{\frac{m}{2},j}^{m,n}\right) & m \text{ even,} \\ \operatorname{diag}\left(\iota\lambda_{1,j}^{m,n}, -\iota\lambda_{1,j}^{m,n}, \iota\lambda_{2,j}^{m,n}, -\iota\lambda_{2,j}^{m,n}, \dots, \iota\lambda_{\lfloor \frac{m}{2} \rfloor,j}^{m,n}, -\iota\lambda_{\lfloor \frac{m}{2} \rfloor,j}^{m,n}, \iota\lambda_{\frac{m+1}{2},j}^{m,n}\right) & m \text{ odd.} \end{cases}$$

The matrix

$$\begin{pmatrix} 2\iota b\cos\frac{\pi}{m+1} & (-1)^{m-1}2\iota^m c\cos\frac{j\pi}{n+1} \\ & \ddots & \ddots \\ & & \ddots & \ddots \\ (-1)^0 2\iota^m c\cos\frac{j\pi}{n+1} & 2\iota b\cos\frac{m\pi}{m+1} \end{pmatrix},$$

when diagonalized, becomes equal to D_j . Thus, F_j becomes similar to

$$(5.3) \quad I_m \otimes \operatorname{diag}\left(x + 2\iota a \cos \frac{\pi}{\ell + 1}, \dots, x + 2\iota a \cos \frac{\ell \pi}{\ell + 1}\right) + D_j \otimes \iota^{\ell - 1} \begin{pmatrix} & & (-1)^{\ell - 1} \\ & & \ddots & \\ & & & (-1)^0 \end{pmatrix}.$$

Again, as the first matrix in both tensor products of (5.3) is diagonal, each block F_j is similar to a block diagonal matrix given by

$$F_{j} \sim \begin{cases} \operatorname{diag}(F_{1,j}^{+}, F_{1,j}^{-}, \dots, F_{\frac{m}{2},j}^{+}, F_{\frac{m}{2},j}^{-}) & m \text{ even,} \\ \operatorname{diag}(F_{1,j}^{+}, F_{1,j}^{-}, \dots, F_{\frac{m-1}{2},j}^{+}, F_{\frac{m-1}{2},j}^{-}, F_{\frac{m+1}{2},j}^{+}) & m \text{ odd,} \end{cases}$$

where

$$F_{s,j}^{\pm} = \operatorname{diag}\left(x + 2\iota a \cos\frac{\pi}{\ell+1}, \dots, x + 2\iota a \cos\frac{\ell\pi}{\ell+1}\right) \pm \iota^{\ell} \lambda_{s,j}^{m,n} \begin{pmatrix} (-1)^{\ell-1} \\ (-1)^{0} \end{pmatrix}$$

$$= \begin{pmatrix} x + 2\iota a \cos\frac{\pi}{\ell+1} & \pm (-1)^{\ell-1} \iota^{\ell} \lambda_{s,j}^{m,n} \\ \vdots & \vdots \\ \pm (-1)^{0} \iota^{\ell} \lambda_{s,j}^{m,n} & x + 2\iota a \cos\frac{\ell\pi}{\ell+1} \end{pmatrix}.$$

Now defining

$$Y_{k,s,j}^{\pm} = \begin{pmatrix} x + 2\iota a \cos\frac{k\pi}{\ell+1} & \pm (-1)^{\ell-k} \iota^l \lambda_{s,j}^{m,n} \\ \pm (-1)^{k-1} \iota^\ell \lambda_{s,j}^{m,n} & x - 2\iota a \cos\frac{k\pi}{\ell+1} \end{pmatrix}, \quad 1 \le s \le \lfloor (m+1)/2 \rfloor,$$

and performing simultaneous row and column interchanges on $F_{s,j}^{\pm}$, we can write

$$F_{s,j}^{\pm} \sim \begin{cases} \operatorname{diag}(Y_{1,s,j}^{\pm}, Y_{2,s,j}^{\pm}, \dots, Y_{\lfloor \frac{\ell}{2} \rfloor, s, j}^{\pm}) & \ell \text{ even,} \\ \operatorname{diag}(Y_{1,s,j}^{\pm}, Y_{2,s,j}^{\pm}, \dots, Y_{\lfloor \frac{\ell}{2} \rfloor, s, j}^{\pm}, \ x \pm \iota \lambda_{s,j}^{m,n}) & \ell \text{ odd.} \end{cases}$$

Note that

$$\det Y_{k,s,j}^+ = \det Y_{k,s,j}^- = x^2 + 4a^2 \cos^2 \frac{k\pi}{\ell+1} + 4b^2 \cos^2 \frac{s\pi}{m+1} + 4c^2 \cos^2 \frac{j\pi}{n+1},$$

which implies that

$$\det F_{s,j}^+ \det F_{s,j}^- = \prod_{k=1}^{\lfloor \ell/2 \rfloor} (\det Y_{k,s,j}^+ \det Y_{k,s,j}^-) \times \begin{cases} 1 & \ell \text{ even,} \\ x^2 + \left(\lambda_{s,j}^{m,n}\right)^2 & \ell \text{ odd.} \end{cases}$$

Then we get,

$$\det F_{j} = \prod_{s=1}^{\lfloor m/2 \rfloor} (\det F_{s,j}^{+} \det F_{s,j}^{-}) \times \begin{cases} 1 & m \text{ even,} \\ \det F_{\frac{m+1}{2},j}^{+} & m \text{ odd.} \end{cases}$$

Hence,

$$\det F_j = \prod_{s=1}^{\lfloor m/2 \rfloor} \prod_{k=1}^{\lfloor \ell/2 \rfloor} \left(x^2 + 4a^2 \cos^2 \frac{k\pi}{\ell+1} + 4b^2 \cos^2 \frac{s\pi}{m+1} + 4c^2 \cos^2 \frac{j\pi}{n+1} \right)^2$$

$$\begin{cases} 1 & \ell, m \in 2\mathbb{N}, \\ \prod_{s=1}^{\lfloor m/2 \rfloor} \left(x^2 + (\lambda_{s,j}^{m,n})^2 \right) & \ell \notin 2\mathbb{N}, m \in 2\mathbb{N}, \\ \prod_{s=1}^{\lfloor \ell/2 \rfloor} \left(x^2 + 4a^2 \cos^2 \frac{k\pi}{\ell+1} + 4c^2 \cos^2 \frac{j\pi}{n+1} \right) & \ell \in 2\mathbb{N}, m \notin 2\mathbb{N}, \\ \prod_{k=1}^{\lfloor \ell/2 \rfloor} \left(x^2 + 4a^2 \cos^2 \frac{k\pi}{\ell+1} + 4c^2 \cos^2 \frac{j\pi}{n+1} \right) & \ell \in 2\mathbb{N}, m \notin 2\mathbb{N}, \\ \times \left(x + 2\iota c \cos \frac{j\pi}{n+1} \right) \prod_{s=1}^{\lfloor m/2 \rfloor} \left(x^2 + (\lambda_{s,j}^{m,n})^2 \right) & \ell, m \notin 2\mathbb{N}. \end{cases}$$

Since, $\det \mathcal{K}_{\ell,m,n} = \prod_{j=1}^n \det F_j$ and $\det F_j = \det F_{n-j+1}$ we obtain the result.

We now make a few remarks about this result. First, the orientation on G is Pfaffian over all standard planes and G is non-planar when at least two of ℓ, m, n are greater than 2. Second, although it is not obvious from Theorem 5.1, $\mathcal{Z}_{\ell,m,n}$ is always a polynomial in x, a, b, c with nonnegative integer coefficients. Third, $\mathcal{Z}_{\ell,m,n}$ is the fourth power of a polynomial when ℓ, m and n are all even and the square of a polynomial when exactly two of ℓ, m and n are even. Fourth, the formula in Theorem 5.1 coincides with the already known partition function [Ayy15] of the monopole-dimer model for the two-dimensional grid graph when either of ℓ, m, n are equal to 1. Finally, although it is not obvious from the construction, the formula is symmetric in all three directions. That is to say, it is symmetric under any permutation interchanging $(a, \ell), (b, m)$ and (c, n).

We now prove that our monopole-dimer model on Cartesian products satisfies an associativity property at least for path graphs.

Proposition 5.3. The partition function of the monopole-dimer model on the oriented Cartesian product of $(P_{\ell} \Box P_m, \mathcal{O}_{\ell,m})$ with (P_n, \mathcal{O}_n) is the same as the partition function of the monopole-dimer model on the oriented Cartesian product of $(P_{\ell}, \mathcal{O}_{\ell})$ with $(P_m \Box P_n, \mathcal{O}_{m,n})$.

Proof. The orientation on both the products is induced from the same boustrophedon labelling given in Remark 5.2. Moreover, the partition function of the monopole-dimer model is the same as the partition function of the loop-vertex model on $P_{\ell} \Box P_m \Box P_n$ with the canonical orientation induced from boustrophedon labelling.

6. Higher-dimensional grid graphs

We now generalise the results from Section 5 to higher dimensional grid graphs. Let us consider d path graphs $P_{m_1}, P_{m_2}, \ldots, P_{m_d}, \ell$ of which are odd. Without loss of generality, we assume that the first ℓ of these are odd, that is m_1, \ldots, m_{ℓ} are odd.

Theorem 6.1. Let (G, \mathcal{O}) be the oriented Cartesian product of the graphs $(P_{m_1} \square P_{m_2}, \mathcal{O}_{m_1, m_2})$, $(P_{m_3}, \mathcal{O}_{m_3}), \ldots, (P_{m_d}, \mathcal{O}_{m_d})$, where m_1, \ldots, m_ℓ are odd. Let vertex weights be x for all vertices of G and edge weights be a_i for the P_{m_i} -edges. Then the partition function of the monopole-dimer model on G is given by

(6.1)
$$\mathcal{Z}_G \equiv \mathcal{Z}_{m_1,\dots,m_d} = \prod_{S \subseteq [\ell]} (T_S)^{2^{d-1-\#S}},$$

where for $S = [d] \setminus \{p_1, \ldots, p_r\},\$

$$T_S = \prod_{i_{p_1}=1}^{\lfloor \frac{m_{p_1}}{2} \rfloor} \cdots \prod_{i_{p_r}=1}^{\lfloor \frac{m_{p_r}}{2} \rfloor} \left(x^2 + \sum_{q=1}^r 4a_s^2 \cos^2 \frac{i_{p_q} \pi}{m_{p_q} + 1} \right),$$

and when $\ell = d$, the empty product in $T_{[d]}$ must be interpreted as x^2 .

Note that if $\ell=d$ then the term in (6.1) corresponding to S=[d] is just x which is expected since each configuration will have at least one monomer. The proof strategy is similar to that of [HM70, Section 4]. Using ideas similar to the proof of Proposition 5.3, it can be shown that for $s \in [d-1]$, the formula above coincides with the partition function of the monopole-dimer model on the oriented Cartesian product $P_{m_1} \square P_{m_2} \square \cdots \square P_{m_{s-1}} \square (P_{m_s} \square P_{m_{s+1}}) \square P_{m_{s+2}} \square \cdots \square P_{m_d}$. We first demonstrate the strategy of proof in an example below.

Example 6.2. Consider the 4-dimensional oriented hypercube, Q_4 , built as an oriented Cartesian product of 4 copies of (P_2, \mathcal{O}_2) as in Definition 3.5. Then the generalised adjacency matrix is

$$\mathcal{K}_G = I_2 \otimes I_2 \otimes I_2 \otimes T_2(-a_1, x, a_1) + I_2 \otimes I_2 \otimes T_2(-a_2, 0, a_2) \otimes J_2 + I_2 \otimes T_2(-a_3, 0, a_3) \otimes J_2 \otimes J_2 + T_2(-a_4, 0, a_4) \otimes J_2 \otimes J_2 \otimes J_2.$$

Let u_k be as defined in the proof of Theorem 5.1. Then, using the unitary transform $u_2 \otimes u_2 \otimes u_2 \otimes u_2$, we see that

$$\mathcal{K}_{G} \sim I_{2} \otimes I_{2} \otimes I_{2} \otimes \begin{pmatrix} x + \iota a_{1} & 0 \\ 0 & x - \iota a_{1} \end{pmatrix} + I_{2} \otimes I_{2} \otimes \begin{pmatrix} \iota a_{2} & 0 \\ 0 & -\iota a_{2} \end{pmatrix} \otimes \iota \begin{pmatrix} 0 & -1 \\ 1 & 0 \end{pmatrix} \\
+ I_{2} \otimes \begin{pmatrix} \iota a_{3} & 0 \\ 0 & -\iota a_{3} \end{pmatrix} \otimes \iota \begin{pmatrix} 0 & -1 \\ 1 & 0 \end{pmatrix} \otimes \iota \begin{pmatrix} 0 & -1 \\ 1 & 0 \end{pmatrix} \\
+ \begin{pmatrix} \iota a_{4} & 0 \\ 0 & -\iota a_{4} \end{pmatrix} \otimes \iota \begin{pmatrix} 0 & -1 \\ 1 & 0 \end{pmatrix} \otimes \iota \begin{pmatrix} 0 & -1 \\ 1 & 0 \end{pmatrix} \otimes \iota \begin{pmatrix} 0 & -1 \\ 1 & 0 \end{pmatrix}.$$

Define, for $1 \leq i_4 \leq 2$,

$$F_{i_4} = I_2 \otimes I_2 \otimes \begin{pmatrix} x + \iota a_1 & 0 \\ 0 & x - \iota a_1 \end{pmatrix} + I_2 \otimes \begin{pmatrix} \iota a_2 & 0 \\ 0 & -\iota a_2 \end{pmatrix} \otimes \iota \begin{pmatrix} 0 & -1 \\ 1 & 0 \end{pmatrix} + \begin{pmatrix} \iota a_3 & (-1)^{i_4 - 1} a_4 \\ (-1)^{i_4} a_4 & -\iota a_3 \end{pmatrix} \otimes \iota \begin{pmatrix} 0 & -1 \\ 1 & 0 \end{pmatrix} \otimes \iota \begin{pmatrix} 0 & -1 \\ 1 & 0 \end{pmatrix},$$

and note that $\det \mathcal{K}_G = \det F_1 \det F_2$. Now

$$F_1 \sim F_2 \sim I_2 \otimes I_2 \otimes \begin{pmatrix} x + \iota a_1 & 0 \\ 0 & x - \iota a_1 \end{pmatrix} + I_2 \otimes \begin{pmatrix} \iota a_2 & 0 \\ 0 & -\iota a_2 \end{pmatrix} \otimes \iota \begin{pmatrix} 0 & -1 \\ 1 & 0 \end{pmatrix} + \begin{pmatrix} \iota \sqrt{a_3^2 + a_4^2} & 0 \\ 0 & -\iota \sqrt{a_3^2 + a_4^2} \end{pmatrix} \otimes \iota \begin{pmatrix} 0 & -1 \\ 1 & 0 \end{pmatrix} \otimes \iota \begin{pmatrix} 0 & -1 \\ 1 & 0 \end{pmatrix},$$

and thus both F_1 and F_2 have same the determinant. Hence $\det \mathcal{K}_G = \det F_1^2$. Iterating the same procedure two more times, we get

$$\det \mathcal{K}_G = \det \begin{pmatrix} x + \iota a_1 & \sqrt{a_2^2 + a_3^2 + a_4^2} \\ -\sqrt{a_2^2 + a_3^2 + a_4^2} & x - \iota a_1 \end{pmatrix}^8.$$

Thus, the partition function of the monopole-dimer model on Q_4 is given by

$$\mathcal{Z}_{Q_4} = (x^2 + a_1^2 + a_2^2 + a_3^2 + a_4^2)^8.$$

Proof of Theorem 6.1. Using Theorem 3.8, the partition function is the determinant of the generalised adjacency matrix, \mathcal{K}_G , of (G, \mathcal{O}) with the boustrophedon labelling, as discussed in Remark 5.2. It will be convenient for us to index the components in the tensor factors in decreasing order. Let

$$M_j^d = \begin{cases} I_{m_d} \otimes \cdots \otimes I_{m_2} \otimes T_{m_1}(-a_1, x, a_1) & j = 1 \\ I_{m_d} \otimes \cdots \otimes I_{m_{j+1}} \otimes T_{m_j}(-a_j, 0, a_j) \otimes J_{m_{j-1}} \otimes \cdots \otimes J_{m_1} & 2 \leq j \leq d, \end{cases}$$

where $T_k(-s,z,s)$ and J_k are defined in the proof of Theorem 5.1. Then \mathcal{K}_G can be written as

(6.2)
$$\mathcal{K}_G = M_1^d + \dots + M_d^d.$$

For $j \in [d]$, define the $m_j \times m_j$ diagonal matrix

$$D_j = \operatorname{diag}\left(2\iota a_j \cos\frac{\pi}{m_j + 1}, \dots, 2\iota a_j \cos\frac{m_j \pi}{m_j + 1}\right)$$

and antidiagonal matrix

$$J'_{j} = \iota^{m_{j}-1} \begin{pmatrix} & & (-1)^{m_{j}-1} \\ & \ddots & \\ (-1)^{0} & & \end{pmatrix}.$$

Let

$$K_j^d = \begin{cases} I_{m_d} \otimes \cdots \otimes I_{m_2} \otimes (xI_{m_1} + D_1) & j = 1\\ I_{m_d} \otimes \cdots \otimes I_{m_{j+1}} \otimes D_j \otimes J'_{j-1} \otimes \cdots \otimes J'_1 & 2 \leq j \leq d. \end{cases}$$

We again use \sim for the equivalence relation on matrices denoting similarity. Let u_k be as defined in the proof of Theorem 5.1. Then, using the unitary transform $u_{m_d} \otimes \cdots \otimes u_{m_1}$, we see that $\mathcal{K}_G \sim K_1^d + \cdots + K_d^d$. Let

$$\lambda_{i_d, i_{d-1}, \dots, i_p} = \sqrt{\sum_{s=p}^d 4a_s^2 \cos^2 \frac{i_s \pi}{m_s + 1}}, 1 \le p \le d.$$

Since the first matrix in each tensor product K_j^d is diagonal, \mathcal{K}_G is similar to an $m_d \times m_d$ block diagonal matrix with the block F_{i_d} , $i_d \in [m_d]$, given by

$$F_{i_d} = K_1^{d-1} + \dots + K_{d-2}^{d-1} + \left(D_{d-1} + 2\iota a_d \cos \frac{i_d \pi}{m_d + 1} J'_{d-1} \right) \otimes J'_{d-2} \otimes \dots \otimes J'_1.$$

Diagonalizing the matrix

$$D_{d-1} + 2\iota a_d \cos \frac{i_d \pi}{m_d + 1} J'_{d-1}$$

leads to the matrix

$$\begin{cases} \operatorname{diag}(\iota\lambda_{i_d,1}, -\iota\lambda_{i_d,1}, \iota\lambda_{i_d,2}, -\iota\lambda_{i_d,2}, \dots, \iota\lambda_{i_d,\lfloor\frac{m_{d-1}}{2}\rfloor}, -\iota\lambda_{i_d,\lfloor\frac{m_{d-1}}{2}\rfloor}) & m_{d-1} \text{ even}, \\ \operatorname{diag}(\iota\lambda_{i_d,1}, -\iota\lambda_{i_d,1}, \iota\lambda_{i_d,2}, -\iota\lambda_{i_d,2}, \dots, \iota\lambda_{i_d,\lfloor\frac{m_{d-1}}{2}\rfloor}, -\iota\lambda_{i_d,\lfloor\frac{m_{d-1}}{2}\rfloor}, 2a_k\iota\cos\frac{i_d\pi}{m_d+1}) & m_{d-1} \text{ odd}. \end{cases}$$

Set $F_{i_d}^+ = F_{i_d}$, $F_{i_d}^- = F_{m_d - i_d + 1}$ for $1 \le i_d \le \lfloor \frac{m_d}{2} \rfloor$, and observe that $F_{i_d}^+ \sim F_{i_d}^-$. Since the determinant of a matrix is invariant under similarity transformation, the partition function can now be calculated as

(6.3)
$$\mathcal{Z}_G = \prod_{i_d=1}^{\lfloor \frac{m_d}{2} \rfloor} (\det F_{i_d}^+)^2 \times \begin{cases} 1 & m_d \text{ even,} \\ \det F_{\underline{m_d+1}} & m_d \text{ odd.} \end{cases}$$

Let us first assume $\ell < d$, i.e. m_d is even. Repeating the above idea, $F_{i_d}^+$ is similar to an $m_{d-1} \times m_{d-1}$ block diagonal matrix with blocks $F_{i_d,i_{d-1}}^\pm$ for $1 \le i_{d-1} \le \lfloor \frac{m_{d-1}}{2} \rfloor$ and continue this process. Inductively, we obtain

(6.4)
$$\mathcal{Z}_G = \prod_{i_d=1}^{\frac{m_d}{2}} \cdots \prod_{i_{\ell+1}=1}^{\frac{m_{\ell+1}}{2}} (\det F^+_{i_d, i_{d-1}, \dots, i_{\ell+1}} \det F^-_{i_d, i_{d-1}, \dots, i_{\ell+1}})^{2^{d-\ell-1}},$$

with

$$F_{i_d,i_{d-1},\dots,i_{\ell+1}}^{\pm} = K_1^{\ell} + \dots + K_{\ell-1}^{\ell} + \left(D_{\ell} \pm \iota \lambda_{i_d,\dots,i_{\ell+1}} J_{\ell}'\right) \otimes J_{\ell-1}' \otimes \dots \otimes J_1'.$$

Again diagonalizing, the matrix

$$D_{\ell} \pm \iota \lambda_{i_d, \dots, i_{\ell+1}} J_{\ell}'$$

is similar to

$$\operatorname{diag}\left(\iota\lambda_{i_d,\dots,i_{\ell+1},1},-\iota\lambda_{i_d,\dots,i_{\ell+1},1},\dots,\iota\lambda_{i_d,\dots,i_{\ell+1},\lfloor\frac{m_\ell}{2}\rfloor},-\iota\lambda_{i_d,\dots,i_{\ell+1},\lfloor\frac{m_\ell}{2}\rfloor},\pm\iota\lambda_{i_d,\dots,i_{\ell+1},\frac{m_\ell+1}{2}}\right).$$

Therefore,

(6.5)
$$\det F_{i_d,i_{d-1},\dots,i_{\ell+1}}^+ = \det F_{i_d,\dots,i_{\ell+1},\frac{m_{\ell+1}}{2}}^+ \prod_{i_{\ell}=1}^{\lfloor m_{\ell}/2 \rfloor} (\det F_{i_d,\dots,i_{\ell+1},i_{\ell}}^+ \det F_{i_d,\dots,i_{\ell+1},i_{\ell}}^-),$$

and

(6.6)
$$\det F_{i_d,i_{d-1},\dots,i_{\ell+1}}^- = \det F_{i_d,\dots,i_{\ell+1},\frac{m_{\ell}+1}{2}}^- \prod_{i_{\ell}=1}^{\lfloor m_{\ell}/2 \rfloor} (\det F_{i_d,\dots,i_{\ell+1},i_{\ell}}^+ \det F_{i_d,\dots,i_{\ell+1},i_{\ell}}^-),$$

where

$$F_{i_d,i_{d-1},\dots,i_{\ell}}^{\pm} = K_1^{\ell-1} + \dots + K_{\ell-2}^{\ell-1} + \left(D_{\ell-1} \pm \iota \lambda_{i_d,\dots,i_{\ell}} J_{\ell-1}'\right) \otimes J_{\ell-2}' \otimes \dots \otimes J_1'.$$

Substituting (6.5) and (6.6) in (6.4) gives

$$\mathcal{Z}_{G} = \prod_{i_{d}=1}^{\frac{m_{d}}{2}} \cdots \prod_{i_{\ell}=1}^{\frac{m_{\ell}}{2}} (\det F_{i_{d},i_{d-1},\dots,i_{\ell}}^{+} \det F_{i_{d},i_{d-1},\dots,i_{\ell}}^{-})^{2^{d-\ell}}$$

$$\prod_{i_{d}=1}^{\frac{m_{d}}{2}} \cdots \prod_{i_{\ell+1}=1}^{\frac{m_{\ell+1}}{2}} \left(\det F_{i_{d},\dots,i_{\ell+1},\frac{m_{\ell}+1}{2}}^{+} \det F_{i_{d},\dots,i_{\ell+1},\frac{m_{\ell}+1}{2}}^{-}\right)^{2^{d-\ell-1}}$$

By repeated application of this procedure, we will get

$$\mathcal{Z}_{G} = \prod_{i_{d}=1}^{\frac{m_{d}}{2}} \cdots \prod_{i_{1}=1}^{\lfloor \frac{m_{1}}{2} \rfloor} (\det F_{i_{d},\dots,i_{1}}^{+} \det F_{i_{d},\dots,i_{1}}^{-})^{2^{d-1}} \prod_{\substack{S \subset [\ell] \\ |S|=1}} T_{S}^{2^{d-2}} \prod_{\substack{S \subset [\ell] \\ |S|=2}} T_{S}^{2^{d-3}} \cdots \prod_{\substack{S \subset [\ell] \\ |S|=\ell}} T_{S}^{2^{d-\ell-1}},$$

where $F_{i_d,...,i_1}^{\pm}$ is the 1×1 matrix

$$\left(\pm \iota \sqrt{x^2 + \sum_{s=1}^d 4a_s^2 \cos^2 \frac{i_s \pi}{m_s + 1}}\right).$$

Thus, we finally arrive at

$$(6.7) \mathcal{Z}_{G} = \prod_{i_{d}=1}^{\frac{m_{d}}{2}} \cdots \prod_{i_{1}=1}^{\lfloor \frac{m_{1}}{2} \rfloor} \left(x^{2} + \sum_{s=1}^{d} 4a_{s}^{2} \cos^{2} \frac{i_{s}\pi}{m_{s}+1} \right)^{2^{d-1}} \prod_{\substack{S \subset [\ell] \\ |S|=1}} T_{S}^{2^{d-2}} \prod_{\substack{S \subset [\ell] \\ |S|=2}} T_{S}^{2^{d-3}} \cdots \prod_{\substack{S \subset [\ell] \\ |S|=\ell}} T_{S}^{2^{d-\ell-1}}.$$

The last case is when $\ell = d$. Then the right hand side of (6.7) will have an additional factor of $\det F_{\frac{m_d+1}{2}}$, and the latter is the generalised adjacency matrix for the oriented Cartesian product $(P_{m_1} \Box P_{m_2}, \mathcal{O}_{m_1, m_2}) \Box (P_{m_3}, \mathcal{O}_{m_3}) \Box \cdots \Box (P_{m_{d-1}}, \mathcal{O}_{m_{d-1}})$. Thus,

$$\det F_{\frac{m_d+1}{2}} = \prod_{S \subseteq [d-1]} (T_S)^{2^{d-2-\#S}} = \prod_{\substack{\emptyset \subsetneq S \subseteq [d] \\ d \in S}} (T_S)^{2^{d-1-\#S}},$$

by induction. Substituting this in (6.3) completes the proof.

As for the three-dimensional case, it is not obvious from the formula (6.1) for $\mathcal{Z}_{m_1,\ldots,m_d}$ that it is a polynomial with nonnegative integer coefficients. The formula is also symmetric under any permutation of $(a_1, m_1), \ldots, (a_k, m_d)$. Finally, (6.1) tells that the partition function of the monopole-dimer model for even grid lengths is the $2^{(d-1)}$ 'th power of a polynomial. Again a combinatorial interpretation of the underlying polynomial would be interesting.

We end this section with an example for a well-studied family of graphs.

Example 6.3. Consider the d-dimensional oriented hypercube, Q_d , built as an oriented Cartesian product of d copies of (P_2, \mathcal{O}_2) as in Definition 3.5. Then the partition function of the monopole-dimer model on Q_d is given by

$$\mathcal{Z}_{Q_d} = (x^2 + a_1^2 + \dots + a_d^2)^{2^{d-1}}.$$

While this formula is amazingly simple, it is a result of a lot of cancellation of terms. Finding a combinatorial interpretation of this formula would certainly be very interesting. An interpretation in the two-dimensional case has been given in [Ayy20].

7. Asymptotic Behaviour

It is natural to ask how fast the partition function of these monopole-dimer models on grid graphs grows as the size increases. We are also interested in understanding the 'probability' of seeing a monopole at a given vertex or a dimer at a given edge. The reason these are not strict probabilities is that we are working with signed measures. As a warm-up, we begin with three-dimensional grids in Section 7.1. We then move on the general d-dimensional grids in Section 7.2, where the formulas are not as explicit. We will follow the strategy in [Ayy15, Section 5].

7.1. Three-dimensional grids. Define the free energy as

$$\Phi_3(a,b,c,x) := \lim_{\ell,m,n\to\infty} \frac{1}{8\ell mn} \ln \mathcal{Z}_{2\ell,2m,2n}.$$

Using the product formula in Theorem 5.1,

$$\Phi_3(a,b,c,x) = \lim_{\ell,m,n\to\infty} \frac{1}{8\ell mn} \times \sum_{j=0}^n \sum_{s=0}^m \sum_{k=0}^\ell \ln\left(x^2 + 4a^2\cos^2\frac{\pi k}{2\ell+1} + 4b^2\cos^2\frac{\pi s}{2m+1} + 4c^2\cos^2\frac{\pi j}{2n+1}\right)^4.$$

Note that the right hand side can be expressed as a Riemann sum. Therefore,

$$\Phi_3(a,b,c,x) = \frac{4}{\pi^3} \int_0^{\pi/2} \int_0^{\pi/2} \int_0^{\pi/2} \ln(x^2 + 4a^2 \cos^2 \theta + 4b^2 \cos^2 \phi + 4c^2 \cos^2 \psi) d\theta d\phi d\psi.$$

Hence, the *density* of a-type edges and of monopoles will be

$$\rho_{3,a} := a \frac{\partial}{\partial a} \Phi_3 = \frac{4}{\pi^3} \int_0^{\pi/2} \int_0^{\pi/2} \int_0^{\pi/2} \frac{8a^2 \cos^2 \theta}{(x^2 + 4a^2 \cos^2 \theta + 4b^2 \cos^2 \phi + 4c^2 \cos^2 \psi)} d\theta d\phi d\psi,$$

$$\rho_{3,x} := x \frac{\partial}{\partial x} \Phi_3 = \frac{4}{\pi^3} \int_0^{\pi/2} \int_0^{\pi/2} \frac{2x^2}{(x^2 + 4a^2 \cos^2 \theta + 4b^2 \cos^2 \phi + 4c^2 \cos^2 \psi)} d\theta d\phi d\psi,$$

respectively. Similarly, the density of b- and c-type dimers can be defined and one can check that $\rho_{3,a} + \rho_{3,b} + \rho_{3,c} + \rho_{3,x} = 1$ as expected.

Recall the elliptic integral of the first kind,

$$F(\phi, k) = \int_{0}^{\phi} \frac{\mathrm{d}\alpha}{\sqrt{1 - k^2 \sin^2 \alpha}},$$

and the elliptic integral of the second kind,

$$E(\phi, k) = \int_{0}^{\phi} \sqrt{1 - k^2 \sin^2 \alpha} \, d\alpha.$$

The complete elliptic integral of the first kind is $K(k) = F(\pi/2, k)$ and the complete elliptic integral of the second kind is $E(k) = E(\pi/2, k)$. Then, the Jacobi zeta function is

$$Z(\phi, k) = E(\phi, k) - \frac{E(k)}{K(k)} F(\phi, k).$$

See Gradshteyn and Rizhik [GR00] for basic properties of elliptic integrals. Now performing similar calculations as in [Ayy15] using

$$\epsilon_3 = \tan^{-1} \left(\frac{\sqrt{x^2 + 4c^2 \cos^2 \psi + 4b^2}}{2a} \right)$$

and

$$q_3 = \frac{4ab}{\sqrt{(x^2 + 4c^2\cos^2\psi + 4a^2)(x^2 + 4c^2\cos^2\psi + 4b^2)}},$$

we get,

(7.1)
$$\rho_{3,a} = 1 - \frac{2}{\pi} \int_{0}^{\pi/2} \Lambda_0(\epsilon_3, \sin^{-1} q_3) d\psi,$$

(7.2)
$$\rho_{3,x} = \frac{x^2}{\pi^2 ab} \int_0^{\pi/2} q_3 K(q_3) d\psi,$$

where $\Lambda_0(\theta, y)$ is the Heuman lambda function [AS64, Formula 17.4.39] defined as

$$\Lambda_0(\theta, y) = \frac{F(\phi, \cos y)}{K(\cos y)} + \frac{2}{\pi}K(\sin y)Z(\phi, \cos y).$$

Let us now calculate the monopole density for the three dimensional case when all the vertex and edge weights are 1. Using (7.2), we get

$$\rho_{3,x} = \frac{1}{\pi^2} \int_{0}^{\pi/2} \frac{4}{5 + 4\cos^2 \psi} K\left(\frac{4}{5 + 4\cos^2 \psi}\right) d\psi \approx 0.1705.$$

7.2. d-dimensional grids. We now move on to the case of d-dimensional grid graphs where all side lengths are even, vertex weights are x and edges along the j'th direction have weight a_j . The free energy is given by

$$\Phi_d(a_1, \dots, a_d, x) := \lim_{m_1, \dots, m_d \to \infty} \frac{1}{2^d m_1 \cdots m_d} \ln \mathcal{Z}_{2m_1, \dots, 2m_d}.$$

The product formula in Theorem 6.1 together with the Riemann sum implies that

$$\Phi_d(a_1, \dots, a_d, x) = \frac{2^{d-1}}{\pi^d} \int_0^{\pi/2} \dots \int_0^{\pi/2} \ln\left(x^2 + \sum_{s=1}^d 4a_s^2 \cos^2 \theta_s\right) d\theta_1 \dots d\theta_d.$$

Again defining the densities of monopoles and s-type edges for $s \in [d]$ as

$$\rho_{d,x} := x \frac{\partial}{\partial x} \Phi_d, \quad \rho_{d,a_s} := a_s \frac{\partial}{\partial a_s} \Phi_d,$$

one can again get that $\rho_{d,x} + \sum_{s=1}^{d} \rho_{d,a_s} = 1$. Following the strategy in [Ayy15], we define

$$\epsilon_d = \tan^{-1}\left(\frac{\sqrt{x^2 + 4a_2^2 + \sum_{s=3}^d 4a_s^2 \cos^2 \theta_s}}{2a_1}\right),$$

$$q_d = \frac{4a_1a_2}{\sqrt{(x^2 + 4a_1^2 + \sum_{s=3}^d 4a_s^2 \cos^2 \theta_s)(x^2 + 4a_2^2 + \sum_{s=3}^d 4a_s^2 \cos^2 \theta_s)}},$$

and we get

$$\rho_{d,a_1} = 1 - \frac{2^{d-2}}{\pi^{d-2}} \int_0^{\pi/2} \cdots \int_0^{\pi/2} \Lambda_0(\epsilon_d, \sin^{-1} q_d) d\theta_3 \dots d\theta_d,$$

$$\rho_{d,x} = \frac{2^{d-3} x^2}{\pi^{d-1} a_1 a_2} \int_0^{\pi/2} \cdots \int_0^{\pi/2} q_d K(q_d) d\theta_3 \dots d\theta_d.$$

Figure 11 shows the numerically evaluated monopole density $\rho_{d,x}$ for the first few dimensions when all the vertex and edge weights are 1. Observe that $\rho_{d,x}$ seems to decrease monotonically as dimension increases. It would be interesting to determine the limit of $\rho_{d,x}$ as d tends to infinity, if it exists. In particular, it is not clear whether this limit is 0 or not.

ACKNOWLEDGEMENTS

We thank the referees for many helpful comments and suggestions.

References

- [AS64] Milton Abramowitz and Irene A Stegun. Handbook of mathematical functions with formulas, graphs, and mathematical tables, volume 55. US Government printing office, 1964.
- [Ayy15] Arvind Ayyer. A statistical model of current loops and magnetic monopoles. *Math. Phys. Anal. Geom.*, 18(1):Art. 16, 19, 2015. URL: https://doi.org/10.1007/s11040-015-9185-6, doi:10.1007/s11040-015-9185-6.

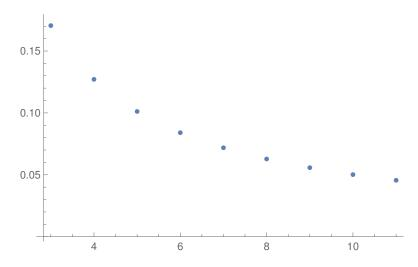


FIGURE 11. Monopole densities $\rho_{d,x}$ for limiting grid graphs in dimensions d ranging from 3 to 11 when all the vertex and edge weights are 1.

- [Ayy20] Arvind Ayyer. Squareness for the monopole-dimer model. Ann. Comb., 24(2):237-255, 2020. URL: https://doi.org/10.1007/s00026-019-00480-5, doi:10.1007/s00026-019-00480-5.
- [BM08] J. A. Bondy and U. S. R. Murty. *Graph theory*, volume 244 of *Graduate Texts in Mathematics*. Springer, New York, 2008. URL: https://doi.org/10.1007/978-1-84628-970-5, doi:10.1007/978-1-84628-970-5.
- [Cay49] A. Cayley. Sur les déterminants gauches. (suite du mémoire t. xxxii. p. 119). Crelle's journal, 1849(38):93–96, 1849. URL: https://doi.org/10.1515/crll.1849.38.93, doi:doi:10.1515/crll.1849.38.93.
- [CSW23] Nishant Chandgotia, Scott Sheffield, and Catherine Wolfram. Large deviations for the 3D dimer model. 2023. arXiv:2304.08468.
- [Fis61] Michael E. Fisher. Statistical mechanics of dimers on a plane lattice. *Phys. Rev.*, 124:1664–1672, Dec 1961. URL: https://link.aps.org/doi/10.1103/PhysRev.124.1664, doi:10.1103/PhysRev.124.1664.
- [GR00] I. S. Gradshteyn and I. M. Ryzhik. Table of integrals, series, and products. Academic Press Inc., San Diego, CA, sixth edition, 2000. Translated from the Russian, Translation edited and with a preface by Alan Jeffrey and Daniel Zwillinger.
- [HLT23] Ivailo Hartarsky, Lyuben Lichev, and Fabio Toninelli. Local dimer dynamics in higher dimensions, 2023. arXiv:2304.10930.
- [HM70] J. M. Hammersley and V. V. Menon. A lower bound for the monomer-dimer problem. J. Inst. Math. Appl., 6:341-364, 1970. doi:10.1093/imamat/6.4.341.
- [Jer87] Mark Jerrum. Two-dimensional monomer-dimer systems are computationally intractable. *Journal of Statistical Physics*, 48(1):121–134, 1987. URL: https://doi.org/10.1007/BF01010403, doi:10.1007/BF01010403.
- [Kas61] P.W. Kasteleyn. The statistics of dimers on a lattice: I. the number of dimer arrangements on a quadratic lattice. Physica, 27(12):1209-1225, 1961. URL: https://www.sciencedirect.com/science/article/pii/0031891461900635, doi:https://doi.org/10.1016/0031-8914(61)90063-5.
- [Kas63] P. W. Kasteleyn. Dimer statistics and phase transitions. *Journal of Mathematical Physics*, 4(2):287–293, 1963. URL: https://doi.org/10.1063/1.1703953, doi:10.1063/1.1703953.
- [TF61] H. N. V. Temperley and Michael E. Fisher. Dimer problem in statistical mechanics-an exact result. The Philosophical Magazine: A Journal of Theoretical Experimental and Applied Physics, 6(68):1061–1063, 1961. URL: https://doi.org/10.1080/14786436108243366, doi:10.1080/14786436108243366.
- [Wu06] F. Wu. Pfaffian solution of a dimer-monomer problem: Single monomer on the boundary. *Physical Review* E, 74(2), 2006. doi:10.1103/PhysRevE.74.020104.

Anita Arora, Department of Mathematics, Indian Institute of Science, Bangalore 560012, India. $Email\ address$: anitaarora@iisc.ac.in

ARVIND AYYER, DEPARTMENT OF MATHEMATICS, INDIAN INSTITUTE OF SCIENCE, BANGALORE 560012, INDIA. $Email\ address$: arvind@iisc.ac.in